Synthesis, Structure, and Bonding Analysis of Lewis Base and Lewis Acid/Base-Stabilized Phosphanylgallanes

T. Ilgin Demirer,[a] Bernd Morgenstern,[a] and Diego M. Andrada*[a]

Phosphanylgallane with hydrogen and halogen substituents (RXGa—PHR, R = organic substituent, X = halogen/hydrogen) are regarded as putative suitable precursors for accessing Ga=P doubly bonded species. Herein, we report on the synthesis, structure, and bonding analysis of a series of Lewis base- and Lewis acid/base-stabilized phosphanylgallane bearing P—H and Ga—Cl/H substitution. To avoid oligomerization, the treatment of $IDip.GaCl_3$ and $(IDip)GaH_2Cl$ (IDip = 1,3-bis(2,6-diisopropyl-phenyl) imidazole-2-ylidene) with LiPHR or $LiPHR(BH_3)$ (R = Ph, Tip, Mes, $NiPr_2$, NCy_2) affords the corresponding Lewis base and Lewis acid/base coordinated H,Cl-functionalized monomeric phosphanylgallane, respectively. The structure of these deriva-tives were determined by spectroscopic and X-ray crystallo-graphic analyses. The observed Ga—P bond lengths are comparable to those previously reported phosphanylgallane analogues. The nature of the C^{IDip}-Ga coordination bond was assessed with Energy Decomposition Analysis, suggesting a relatively stable adduct. Reactions of the phosphanylgallane with Brønsted bases were investigated.

Introduction

Unsaturated main group compounds containing a combination of heavier group 13 (E^{13}) and group 15 (E^{15}) elements are interesting precursors for preparing binary materials with applications in opto- and microelectronic devices.[1] The pre-established 1:1 relationship between these elements has driven captivating investigations to prove their value as single source precursors using metal-organic chemical vapour deposition (MOCVD) or molecular beam epitaxy (MBE) methods.[2] The intended $E^{13}=E^{15}$ functional groups are isoelectronic to C=C in alkenes, but their electronegative difference provides a marked tendency to form dimers, trimers, or tetramers (Scheme 1A). Nonetheless, particular interest has been placed on synthesizing monomeric $[R_2E^{13}=E^{15}R_2]$ species, over the oligomers, because of their increased volatility and potentially simple deposition process.[3]

In contrast to the lightest $E^{13}=E^{15}$ combination (B=N), their heavier congeners like Al=P or Ga=P have a significantly weak π-bond, making the monomeric forms synthetically challenging.[4] A common stabilization strategy involves the use of sterically demanding organic substituents around the double bond, which provides kinetic and thermodynamic stability, but inevitably decreasing volatility.[5] Another strategy is based on the stabilization provided through a Lewis base and/or acid
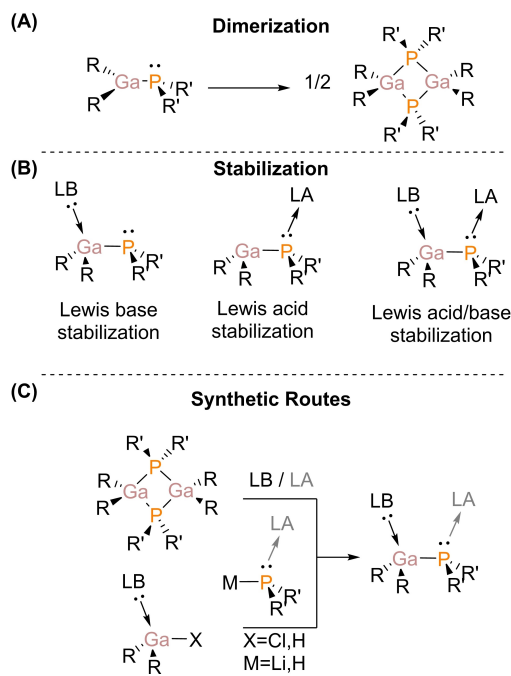
Scheme 1. Phosphagallanes as example of group 13/15 multiple bonded compounds: (A) dimerization process, (B) different types of stabilization, (C) synthetic routes followed for the synthesis of monomeric species. LA = Lewis acid, LB = Lewis base, R = organic substituent.

coordination, which essentially blocks the empty p-orbital on E^{13} or the lone pair at E^{15} elements (Scheme 1B).[6]

The oligomeric heterocycles have served as starting com-pounds for the generation of their monomeric forms (Scheme 1C).[3,7] Despite some Lewis base stabilized adducts have been reported in the past (Scheme 2, **I**), Schulz and co-workers have introduced a general straightforward synthetic route towards the monomeric species via E^{13}-E^{15} bond cleavage of the heterocycle with DMAP (4-dimethylamino-pyridine) as a

[a] T. I. Demirer, Dr. B. Morgenstern, Dr. D. M. Andrada
Faculty of Natural Sciences and Technology, Department of Chemistry
Universität des Saarlandes
Campus C4.1, 66123 Saarbrücken, Germany
E-mail: diego.andrada@uni-saarland.de
http://inorg-comp-chem.com/
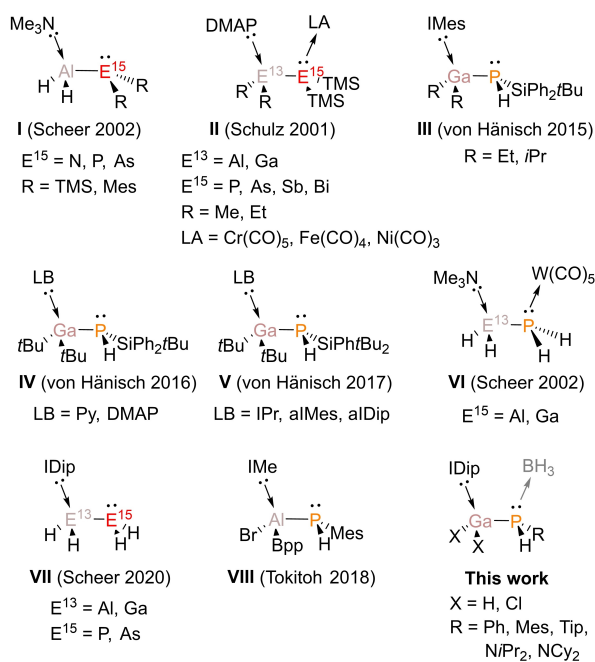
Scheme 2. Previously reported examples of Lewis stabilized group 13/15 species. Py = pyridine, DMAP = 4-dimethylamino-pyridine, IMe = 1,3,4,5-tetra methyl imidazole-2-ylidene, IPr = 1,3-diisopropyl-4,5-dimethylimidazole-2-ylidene, IMes = 1,3-bis-(2,4,6-trimethylphenyl) imidazole-2-ylidene, IDip = 1,3-bis(2,6-diisopropylphenyl) imidazole-2-ylidene, aIMes = abnormal IMes, aIDip = abnormal IDip, Mes = 2,4,6-Me$_3$C$_6$H$_2$, Tip = 2,4,6-iPr$_3$C$_6$H$_2$, Bbp = 2,6-[CH-(SiMe$_3$)$_2$]$_2$C$_6$H$_3$.

Diego M. Andrada studied chemistry at the National University of Córdoba, Argentina, where he obtained his PhD degree under the supervision of Prof. Alejandro M. Granados. In 2012, he joined the group of Prof. Ricardo A. Mata at the Georg-August University of Göttingen, Germany. After a second postdoctoral stay at Philipps-University of Marburg with Prof. Gernot Frenking, he initiated his independent research career in 2018 at Saarland University. His research group focuses on the chemistry main group unsaturated compounds and the chemical bonding concepts.

Lewis base (Scheme 1C first reaction).[8] With many examples, monomeric species (**II**) containing Al—P and Ga—P units have been isolated and characterized with this strategy, even involving a coordination transition metal on E^{15}.[9] However, not all the Lewis bases are able to cleave the heterocycles by coordinating the E^{13}. The group of von Hänisch has addressed a thorough study to determine the limitations of the Lewis base stabilization for Ga—P-containing molecules.[10] They have prepared monomeric species of galliumsilylphosphanide derivates for relatively small substitutions on the Ga atom using the strong Lewis base IMes (1,3-bis-(2,4,6-trimethylphenyl)imidazole-2-ylidene, **III**).[10e] Their attempts to create a doubly bonding Ga=P by thermal-induced elimination reactions resulted in the formation of heterocubane structure, pointing

out the need for more demanding steric protection. However, when the substituents on Ga are bulkier, they observed that using a strong σ-donor Lewis base is not enough to cleave the oligomeric heterocycle when the steric demand is high. Thus, pyridine, DMAP and IPr (1,3-diisopropyl-4,5-dimethylimidazole-2-ylidene) can coordinate (**IV**).[10c] Only IMes and IDip can provide such stabilization after a rearrangement if the group at the phosphorous terminal is large (**V**).[10a]

A different approach has been employed by the group of Scheer, which essentially bypasses the generation of the heterocycle by directly reacting the corresponding adduct by salt, dihydrogen, and alkane elimination reactions, furnishing the Lewis base or Lewis acid/base pair compounds directly.[11] In this manner, Scheer and co-workers synthesized several unsubstituted group 13/15 compounds, for instance (**VI**).[11–12] Notably, this strategy allows the use of bulky NHC-stabilized gallium chlorides, hydrochlorides, and hydrides,[13] giving access to the smallest stabilized phosphanylalanes and phosphanylgallanes (**VII**).[12e]

The NHC as Lewis bases are very interesting not only for the stabilization provided on the group 13 element but also to enforce multiple chemical bonds in some cases.[14] The group of Rivard has provided a detailed description of the synthesis of amido- and azide-functionalized gallium hydrides as potential precursors for Ga≡N compounds.[15] Recently, Tokitoh and co-workers have explored HBr elimination from Lewis base stabilized sterically hindered phosphanylalumane adduct (**VIII**).[16] Herein, we report the synthesis of Lewis base and Lewis acid/base stabilized *H,H*-, and *H,Cl*-functionalized phosphanylgallane. Furthermore, we assess their reactivity toward bases and the effect of the substituents at gallium and phosphorous sites on the overall stability of the monomeric compounds. These adducts have been fully characterized, and their electronic structures have been described by theoretical calculations.

Results and Discussion

We have selected the strong σ-donor Lewis base 1,3-bis(2,6-diisopropylphenyl) imidazoline-2-ylidene (IDip) since it has been demonstrated its value to provide thermodynamic and kinetic stability to phosphagallanes.[12e] Thus, we started our investigation by reacting LiPPh$_2$ with the Lewis base-stabilized trichloro-(IDip.GaCl$_3$) and mono-chlorogallane adducts (IDip.GaH$_2$Cl) in THF at −78 °C. These reactions afforded the mono substituted compounds **3** and **4**. The crystals can be isolated as a white solid stable at room temperatures in an inert atmosphere with yields of 34 %(**3**) and 21 % (**4**). The low yields are a consequence of the IDip elimination, similarly to the observations reported elsewhere.[12e] ^{1}H NMR spectrum of compound **4** shows a doublet at 4.2 ppm ($^2J_{P,H}$ = 13.3 Hz) for the GaH$_2$-unit, while the ^{31}P NMR spectrum gives a broad singlet at −59.1 ppm. This value is slightly upfield shifted compared to the dicyclohexylphophane analogue reported by the group of Scheer (−56.1 ppm).[12e] The chlorinated congener compound **3** shows a downfield shifted phosphorus chemical shift (−51.7 ppm), compared to hydride phophagallane **4** (Scheme 3.

EurJIC
European Journal of Inorganic Chemistry

Research Article
doi.org/10.1002/ejic.202200477

Chemistry
Europe
European Chemical
Societies Publishing
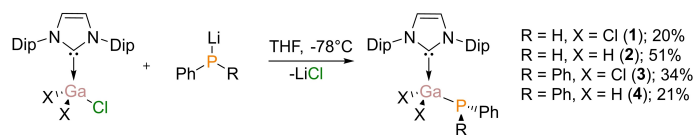
Scheme 3. Synthesis of compounds **1–4**.

Figure 1. Molecular structures of Lewis base-stabilized phosphanylgallane compounds **1** (a), **2** (b), **3** (c), and **4** (d). Ellipsoids set at 50 % probability level. Hydrogen atoms, with the exception of those attached to gallium and phosphorous atoms, are omitted for clarity.

Likewise, with the aim to prepare the precursors for generating monomeric Lewis base stabilized phosphagallene compounds bearing Ga=P, we followed with the synthesis of 1,2 *H,H/H,Cl*-functionalized phosphanylgallane **1** and **2** analogues. The reactions have been carried out in a similar fashion as with compounds **3** and **4**. Treatment of LiHPPh with IDip gallium hydrochlorides and chlorides adduct afforded products **1** and **2** in poor to moderate yields. The compounds were immediately isolated since longer reaction times led to an increasing amount of free IDip in the mixture together with unidentified side products. The ^1H NMR spectrum of **1** and **2** shows a doublet at 2.66 ppm ($^1J_{P,H} = 196.6$ Hz) and a doublet of triplets at 2.8 ($^2J_{H,P} = 188.7$ Hz, $^3J_{H,H} = 4.5$ Hz) for the PH moiety, respectively. In the case of compound **2**, the signal corresponding to the GaH_2 moiety cannot be observed. The ^{31}P NMR spectrum reveals a doublet at −130.3 ppm ($^1J_{P,H} = 197.0$ Hz) and a doublet of triplets at −142.9 ppm ($^1J_{P,H} = 189.6$ Hz, $^2J_{P,H} = 16.4$ Hz) for compound **1** and **2**, respectively. Additionally, the $^{13}C\{^1H\}$ NMR spectra of all compounds **1–4** exhibit a doublet at 168.1 (**1**), 179.2 (**2**), 168.3 (**3**), and 178.8 (**4**) ppm assigned to the carbene carbon coordinated to the Ga center, which is high-field shifted compared to free IDip (220.6 ppm)[17] and in good agreement with previously reported (IDip.GaH₃ 205.9 ppm, IDip.GaH₂Cl 181.6 ppm and IDip.GaHCl₂ 167.9 ppm).[13c]

The IR spectra of compounds **2** and **4** display a strong, broad absorbance at 1825 and 1809 cm⁻¹ (Figures S30 and S32 in the ESI), respectively, which are ascribed to the Ga–H stretching vibrational mode. These values are in good agreement with previously reported gallane adducts NMe₃.GaH₃ (1853 cm⁻¹),[18] IPr.GaH₃ (1775 cm⁻¹, IPr),[19] IDip.GaH₃ (1790 cm⁻¹), and IDip.GaH₂Cl (1877 cm⁻¹).[13c] Notably, it has been suggested elsewhere that lower wavenumbers reflect a stronger donation from the Lewis base.[19]

The solid-state structures of **1–4** were determined by single-crystal X-ray diffraction. Figure 1 shows the molecular structure, and the most important structural features are summarized in Table 1. The obtained Ga–P bond lengths are close to the sum of covalent radii (2.35 Å)[20] and in accordance with the other representative adducts, i.e. IDip.GaH₂PCy₂ (2.3724(6) Å), IDip.GaH₂PH₂ (2.3373(6) Å),[12e] and IMes.GaEt₂P(H)Si*t*BuPh₂ (2.4051(2) Å).[10e] The Ga–C bond lengths are noticeably longer than the expected values for a single bond (Ga–C 1.99 Å).[20] Moreover, these bond lengths are within the range of previously reported gallium complexes IDip.GaH₃ (2.076(2) Å), IDip.GaHCl₂ (2.034(2) Å),[13c] IDip.GaH₂PCy₂ (2.090(2) Å), and IDip.GaH₂PH₂ (2.0507(2) Å),[12e] but slightly shorter than the IMes.GaEt₂P(H)Si*t*BuPh₂ (2.1254(7) Å).[10e]
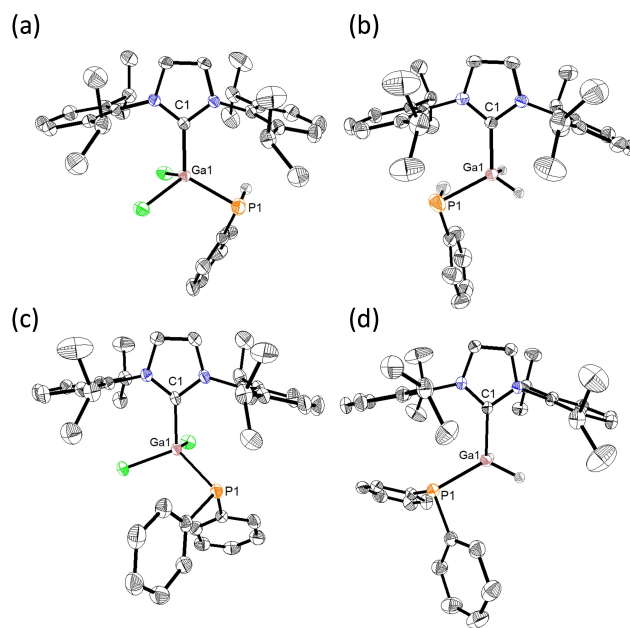
Table 1. Selected experimental and theoretical bond lengths (Å) and angles (°) for compounds **1–8**.[a]				
Ga–C_carb	Ga–P	P–B	$\Sigma\angle$Ga[b]	$\Sigma\angle$P[b]
1 2.032(2)	2.3258(6)	—	325.2	281.2
(2.082)	(2.352)		(331.1)	(286.3)
2 2.057(2)	2.334(1)	—	330.9	245.4
(2.100)	(2.395)		(343.0)	(292.7)
3 2.047(2)	2.3438(7)	—	328.0	304.3
(2.129)	(2.388)		(328.6)	(310.2)
4 2.069(1)	2.3738(4)	—	338.5	307.0
(2.139)	(2.407)		(340.7)	(309.1)
5 2.042(2)	2.3547(6)	1.933(2)	326.8	322.6
(2.072)	(2.369)	(1.944)	(324.7)	(312.8)
6 2.042(3)	2.353(1)	1.935(6)	328.3	322.6
2.116(6)	2.29(1)	1.91(2)	323.9	319.2
(2.078)	(2.386)	(1.938)	(318.3)	(306.6)
7 2.060(1)	2.3694(3)	1.959(2)	336.5	318.6
(2.076)	(2.392)	(1.988)	(335.8)	(303.8)
8 2.052(2)	2.3739(5)	1.954(2)	337.6	314.8
(2.089)	(2.405)	(1.974)	(338.6)	(311.3)

[a] All calculations were performed at the B3LYP-D3(BJ)/def2-SVP level of theory. [b] Sum of angles around Ga/P atom, disregarding the Lewis Acid or Base molecule.

The coordination of the Lewis base results in a different degree of pyramidalization of the gallium atom depending on the substituents, being the chlorinated adducts those with the lower sum of bond angles: 325.2 (**1**), 330.9 (**2**), 328.0 (**3**), and 336.5 (**4**). In the same vein, the phosphorus atoms are also pyramidal 281.2 (**1**), 245.4 (**2**), 304.3 (**3**), and 307.0 (**4**), which suggest that the coordination with the Lewis base precludes optimal π-conjugation.

To gain deeper insight into the electronic structure of compounds **1–4**, we carried out DFT calculations at the B3LYP-

EurJIC
European Journal of Inorganic Chemistry

Research Article
doi.org/10.1002/ejic.202200477

Chemistry Europe
European Chemical
Societies Publishing

D3(BJ)/def2-SVP level of theory (see Computational Details). The optimized geometries are in good agreement with the experimentally determined structures, as summarized in the Table 1. As a general observation, the computed bond lengths are slightly longer than the experimental ones.[21] Inspection of the frontier Kohn-Sham molecular orbitals (KS-MO) identifies the HOMO as the lone pair located at the phosphorus atom, while LUMO is located at the π-system of the IDip ligand (Figures S38-S41 in the ESI).

We analyzed the electronic structures of **1–4** by Natural Bond Orbitals (NBO) analysis.[22] Table 2 gathers the calculated natural atomic partial charges (Q) and Wiberg bond orders (P) of the Ga-C_{carb} and Ga–P bonds calculated at the B3LYP-D3(BJ)/def2-TZVPP level of theory on the previous optimized geometries. The localization of the orbitals shows the presence of a polarized Ga–P σ-bonds (Figures S46-S49). The contribution of phosphorous is between 66.07% and 70.41%, which is expected from Pauli electronegativities. (Ga: 1.41, P: 2.19).[23] As a comparison, the aluminium analogues bear slightly more polarized bond i.e. 74 to 77% contribution of the phosphorus atom.[7] Additionally, there is a lone pair (LP) on the phosphorus atom with p-character of around 50%, which is in agreement with the pyramidalization observed in the crystal structures. Natural population analyses (NPAs) indicate a positive charge of ca. +0.60e on the Ga atom for the hydride derivatives, while chlorinated compounds bear a positive charge of about +1.10e (Table 2). The charge on the full carbene moiety (Q(IDip)) reveals no significant differences on electron density donated, i.e. about +0.30 e. Notably, the WBI between the gallium and the carbene carbon is slightly higher for **2** (0.54 au) and **4** (0.54 au) than for **1** (0.48 au) and **3** (0.49 au), in contrast to the expected from the comparison in of experimental bond lengths (Table 1).

We also analyzed the electron density distribution with atoms in molecules (QTAIM) using the B3LYP-D3(BJ)/def2-TZVPP electron density.[24] The Laplacian distribution $\nabla^2\rho(r)$ in the C_{carb}–Ga–P plane is depicted in Figure 2b for compounds **3** and **4**. The Laplacian plot shows an electron accumulation on the phosphorus atom localized on the σ-system and the electron density of the Ga–P bond critical point ($\rho^{BCP} = 0.54/0.51$ e/Å³), which is shifted towards the P. In the case of the IDip-Ga the Laplacian distribution suggest a rather ionic bond with the electron density of the bond critical point ($\rho^{BCP} = 0.55/0.52$ e/Å³). A similar picture is observed for the remaining series of compounds (Figure S54).
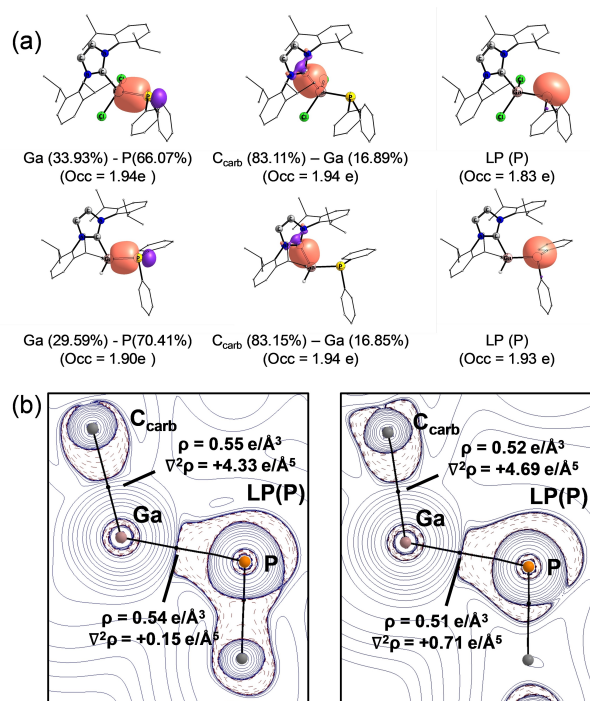
Figure 2. Bonding analysis of **3** and **4** (B3LYP-D3(BJ)/def2-TZVPP//B3LYP-D3(BJ)/def2-SVP). (a) NBOs. (b) 2D Laplacian distribution $\nabla^2\rho(r)$ in the P–Ga-C_{carb} plane. Dashed red lines indicate areas of charge concentration ($\nabla^2\rho(r) < 0$) while solid blue lines show areas of charge depletion ($\nabla^2\rho(r) > 0$), bond paths (black lines), and bcps (black dots).

To examine the strength of the IDip-Ga bonds in series of compounds **1–4**, we have computed and compared the dissociation energies (D_e). Table 3 gives the bond energies at the BP86-D3(BJ)/TZ2P//B3LYP-D3(BJ)/def2-SVP level of theory. These computed bond dissociation energies suggest a relatively strong coordination of the Lewis base ligands to the phosphanylgallane moiety, which is comparable to those values computed for the carbene-alane compounds.[7,12e,25] The values range from 45.5 kcal/mol (**4**) to 57.8 kcal/mol (**1**), being the chlorinated complexes those with larger dissociation energy values. More detailed information about the nature of the chemical bond is provided by the results of the Energy Decomposition Analysis (EDA) method.[21] EDA has proven to be a useful tool to assess the nature of the chemical bond in main group compounds and transition metal compounds.[26] None-

Table 2. Natural Partial Charges (q in a.u.) and Wiberg bond orders (P in a.u.) of all compounds (**1–8**) at the B3LYP-D3(BJ)/def2-TZVPP//B3LYP-D3(BJ)/def2-SVP level of theory.

	Q(P)	Q(Ga)	Q(IDip)	P (Ga–P)	σ(Ga–P) contribution	P (C_{carb}–Ga)	σ(C_{carb}–Ga) contribution
1	−0.03	1.13	0.29	0.79	Ga (33.93%)–P(66.07%)	0.48	C_{carb} (83.11%)–Ga (16.89%)
2	−0.02	0.62	0.29	0.78	Ga (29.59%)–P(70.41%)	0.54	C_{carb} (83.15%)–Ga (16.85%)
3	0.25	1.12	0.30	0.78	Ga (33.23%)–P(66.77%)	0.49	C_{carb} (82.51%)–Ga (17.49%)
4	0.26	0.60	0.31	0.78	Ga (30.50%)–P(69.50%)	0.54	C_{carb} (82.79%)–Ga (17.21%)
5	0.73	1.13	0.30	0.71	Ga (30.59%)–P(69.41%)	0.49	C_{carb} (82.44%)–Ga (17.56%)
6	0.73	1.11	0.33	0.71	Ga (31.00%)–P(69.00%)	0.50	C_{carb} (81.86%)–Ga (18.14%)
7	0.45	0.64	0.33	0.72	Ga (26.18%)–P(73.82%)	0.56	C_{carb} (82.14%)–Ga (17.86%)
8	0.47	0.63	0.33	0.73	Ga (26.67%)–P(73.33%)	0.56	C_{carb} (82.06%)–Ga (17.94%)

EurJIC
European Journal of Inorganic Chemistry

Research Article
doi.org/10.1002/ejic.202200477

Chemistry Europe
European Chemical
Societies Publishing

Table 3. EDA-NOCV results of the C_{carb}-Ga bond in Lewis Base and Lewis Acid/Base-stabilized phosphanylgallanes **1–8** at BP86-D3(BJ)/TZ2P.[a] All values are in kcal/mol.

	1	2	3	4	5	6	7	8
ΔE_{int}	−72.8	−62.3	−75.8	−60.7	−78.3	−77.2	−77.2	−73.7
ΔE_{Pauli}	157.2	126.0	136.9	116.3	173.9	168.5	140.2	131.0
ΔE_{elst}[b]	−125.8 (55%)	−107.0 (57%)	−111.2 (52%)	−93.2 (53%)	−133.9 (53%)	−128.9 (52%)	−117.6 (54%)	−112.7 (55%)
ΔE_{orb}[b]	−77.0 (33%)	−60.0 (32%)	−72.9 (34%)	−59.4 (34%)	−85.1 (34%)	−85.9 (35%)	−69.1 (32%)	−65.8 (32%)
ΔE_{disp}[b]	−27.3 (12%)	−21.3 (11%)	−28.5 (12%)	−24.5 (13%)	−33.2 (13%)	−30.9 (13%)	−30.7 (14%)	−26.2 (13%)
$\Delta E_{prep\ GaP}$	11.6	10.2	14.3	7.1	11.1	13.9	11.4	19.2
$\Delta E_{prep\ IDip}$	3.4	1.8	6.3	3.5	3.6	3.9	2.4	2.2
$\Delta E_{prep\ tot}$	15.0	12.0	20.6	10.6	14.7	17.8	13.8	21.4
$-D_e$	−57.8	−50.3	−55.1	−45.5	−63.6	−59.5	−63.4	−52.3

[a] All calculations were performed on the B3LYP-D3(BJ)/def2-SVP optimized structures. [b] The percentage values in the parentheses give the contribution to the total attractive interactions $\Delta E_{elst} + \Delta E_{orb} + \Delta E_{disp}$.

theless, a recent discussion has been placed about the path function nature of the energy components.[26c,27] Within the EDA scheme, the interaction energy (ΔE_{int}) between two (or more) structurally and electronically unrelaxed fragments of a molecule is divided into four physical meaningful terms, namely, Pauli repulsion (ΔE_{Pauli}), electrostatic interaction (ΔE_{elst}), orbital interaction (ΔE_{orb}), and dispersion interaction (ΔE_{disp}). The dissociation energy is related to the interaction energy by the preparation energy (ΔE_{prep}), which is the energy needed to promote the fragments from their equilibrium geometry to the geometry and electronic state in the compounds.

Table 3 summarizes the numerical results of the EDA calculations performed for the heterolytic fragmentation resulting in IDip and the monomeric phosphagallane. The interaction energies ΔE_{int} follows the same trend as the dissociation energy, leading to stronger interaction for compounds **1** and **3** than for compounds **2** and **4**. The preparation (ΔE_{prep}) of IDip does not carry particular energy penalties as the geometry is rather rigid, giving similar results along the series. The phosphagallanes moieties instead request more energy as a consequence of the pyramidalization of the gallium atom upon coordination. The dissection of the ΔE_{int} reveals that the bonding interactions are on average > 50% ionic with an important contribution of the dispersion interaction > 10%. Noteworthy, the orbital interaction values are higher for **1** and **3** than **2** and **4** by about 10 kcal/mol, given the higher effective acidity,[28] which is partially compensated by the stronger Pauli repulsion.

We attempted to promote the formation of the Lewis base coordinated phosphagallene compounds bearing a Ga=P double, by reacting Brønsted bases with **1** and **2**. However, all attempted reactions to induce elimination of HCl or H_2 by the addition of bases such as NEt_3, morpholine, $K[N(SiMe_3)_2]$, and DBU (1,8-diazabicyclo[5.4.0]undeca-7-ene) were unsuccessful in the regard that no abstraction reaction was observed. Instead, either no reaction (NEt_3) or decomposition with the formation of phosphaalkene (IDipPH), as observed by Blum et al.[29] In order to further corroborate the inertness towards deprotonation, we have computed the proton affinity of compound **1–2**. Previous studies have shown that the proton affinities (PA) are sensitive probe for the presence of chemically available or accessible lone pairs of a molecule.[30] Scheme 4 gathers the calculated PAs of **1–2** at the B3LYP-D3(BJ)/def2-SVP level of
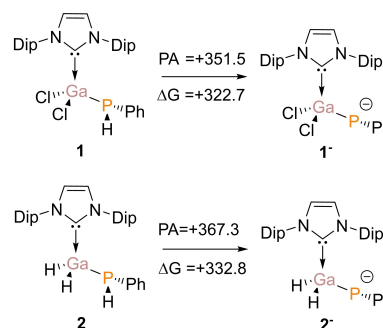
Scheme 4. Calculated Proton Affinities (in kcal/mol) and Gibbs energy (in THF) of compounds **1–2**. DFT calculations were performed at the B3LYP-D3(BJ)/def2-SVP level of theory.

theory. The PA of all compounds are higher than 350 kcal/mol which suggest a highly basic nature of the elusive anion. Note that the calculated PA values follow the trend of the gallium Lewis acidity. The highest PA is for **2** (367.3 kcal/mol), while for **1** the PA is still high but there is a notable reduction of about 15 kcal/mol leading to 351.5 kcal/mol. In terms of Gibbs energy considering the solvent polarity (THF), the deprotonation is endergonic by 322.7 (**1**) and 332.8 (**2**) kcal/mol, which is comparable to the values computed by Agou and coworkers for the Lewis base stabilized phosphanylalumane congeners (**VIII**),[16a] i.e 323.3 kcal/mol.

Since the phosphorus atom of compound **1–4** bears a lone pair, we became interested to elucidate whether the HCl or H_2 elimination of phosphagallane compounds can be accessed by coordinated with a Lewis acid. Thus, we conducted the reaction of $IDip.GaH_2Cl$ and $IDip.GaCl_3$ with the mono-lithiated phosphine-boranes ($RPHLi.BH_3$)[31] in THF at −78 °C afforded the compounds **5–8** (Scheme 5). The compounds were isolated immediately upon the addition of $RPHLi.BH_3$, since longer reaction times leads to an increasing among of free phosphine H_2PR.

Compounds **5–8** were obtained as colourless crystalline solids, which are stable for weeks under inert gas atmosphere at ambient temperature, but they decompose rapidly when exposed to air. Indeed, the formation of side products are observed at short reaction scales for the compound **8**. All compounds were fully characterized by multinuclear NMR, elemental analysis, and IR spectroscopy. The ^1H NMR spectra

Eur. J. Inorg. Chem. **2022**, e202200477 (5 of 10)

© 2022 The Authors. European Journal of Inorganic Chemistry published by Wiley-VCH GmbH

EurJIC
European Journal of Inorganic Chemistry

Research Article
doi.org/10.1002/ejic.202200477

Chemistry Europe
European Chemical Societies Publishing
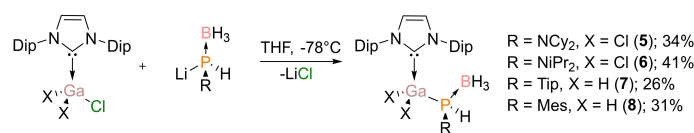
Scheme 5. Synthesis of compounds **5–8**.

exhibit two sets of resonances for the Dip groups for all compounds. Additionally, the PH moiety in **5** and **6** can be detected as doublet of quadruplets at 5.32 ($^1J_{H,P} = 339.8$ Hz, $^3J_{H,H} = 7.3$ Hz) and 5.3 ($^1J_{H,P} = 337.0$ Hz, $^3J_{H,H} = 7.3$ Hz), respectively. The same functionally appears as a doublet of multiplet for **7** at 5.4 ($^1J_{H,P} = 310.2$ Hz, $^3J_{H,H} = 7.0$ Hz), while **8** undergoes decomposition during NMR measurements. The phosphorous chemical shift is in general low-field shifted in comparison to compounds **1–4**. The ^{31}P NMR spectra display broad doublets at -2.9 ($^1J_{P,H} = 342.4$ Hz), -6.71 ($^1J_{P,H} = 339.1$ Hz), -110.7 ($^1J_{P,H} = 309.4$ Hz), and -103.5 ($^1J_{P,H} = 316.8$ Hz) for compound **5**, **6**, **7**, and **8**, respectively. For all compounds, boron atoms appear in the ^{11}B NMR spectra as broad singlets in the range of -34.1 and -35.1 ppm.

In the IR spectra, both P–H and Ga–H stretching bands can be detected as in the case of compounds **1–4**. The Ga–H stretching vibrations of **7** and **8** are observed at higher wavenumbers than compound **2** and **4**, i.e. 1869 and 1871 cm^{-1}. According to the discussion elsewhere this can be associated to a weaker coordination of IDip.[19]

The molecular structures of the compounds **5–8** were confirmed by single crystal X-ray diffraction. Figure 3 displays
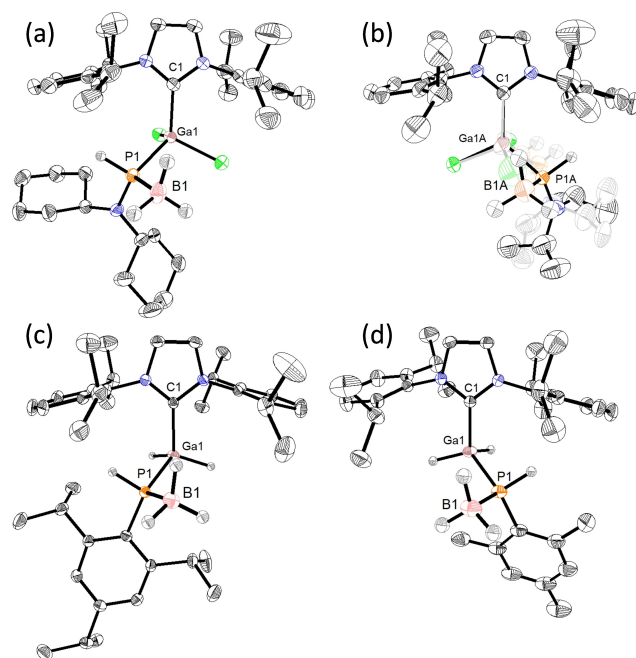
the molecular structure and Table 1 collects the most important structural parameters. The Lewis acid/base coordinated phosphagallane adducts possess a comparable degree of gallium atom pyramidalization with values of 326.6° (**5**) to 337.5° (**8**), while the phosphorus atom shows less pyramidalization leading to wider sum of angles, i.e. 314.6° (**8**) to 322.6 (**6**). The Ga–P bond lengths are in general longer for **5–8** than **1–4**, indicating the absence of π-conjugation. At the same time, the C$_{carb}$–Ga bond length is slightly shorter when the Lewis acid is incorporated, suggesting a stronger coordination as a consequence of the push-pull effect of the Lewis pair.[32]

It is interesting to remark the importance of the substituent on the phosphorus terminal. We attempted to prepare less sterically protected Lewis acid/base phophagallane compounds such as R = Ph or tBu. However, the desired products could not be isolated. Upon addition of the RPHLi.BH$_3$, mixture of compounds including IDip.GaX$_2$PHR.BH$_3$, IDip.GaX$_2$PHR and H$_2$PR were detected in the reaction mixture. Longer reaction times indeed does not lead to full conversion, instead decomposition product into free phosphine is observed. This indicates that the stability of the adducts are highly influenced by the Lewis acidity of the phosphorus, which is enhanced by the presence of the nitrogen of NCy$_2$ and NiPr$_2$ functional groups in compound **5** and **6**.[33] Alternatively, Mes and Tip groups provides enough kinetic stability for isolation, however, decomposition is observed in solution.

Next, we have carried out DFT calculations to examine the electronic structure effects produced by the Lewis acid incorporation. The results are summarized in Table 2 and Table 3. The atomic partial charges show no significant effect on the gallium atom with a value of about $+1.10$ and $+0.60$ e for the chlorinated and hydride derivatives, respectively. As expected, the coordination to BH$_3$ results in a phosphorus atom bearing more positive charge. The Wiberg bond indices indicate a small reduction of the Ga–P bond order together with an increase in the polarization. Additionally, the coordination of IDip to the gallium atom is not significantly affected in polarization of bond order terms. We have applied EDA to gain insight into the coordination strength origins. The bond dissociation energy is in average 5 kcal/mol stronger for the Lewis acid/base pair adducts than for the Lewis base ones. This is reflected in the interaction energy (ΔE_{int}) rather than in the preparation energy (ΔE_{prep}). The Lewis acid incorporation increases mainly the electrostatic and orbital interaction, which is also partially compensated the higher Pauli repulsion.

The calculation of the proton affinity and Gibbs free energy of compound **5–8** are in agreement with the increase of the PH acidity. The Lewis acid coordination represent a lowering of

Figure 3. Molecular structures of Lewis acid/base-stabilized phosphanylgallane compounds **5** (a), **6** (b), **7** (c), and **8** (d). Ellipsoids set at 50% probability level. Hydrogen atoms, with the exception of those attached to gallium and phosphorous atoms, are omitted for clarity.

EurJIC
European Journal of Inorganic Chemistry

Research Article
doi.org/10.1002/ejic.202200477

Chemistry Europe
European Chemical Societies Publishing

Scheme 6. Calculated Proton Affinities (in kcal/mol) and Gibbs energy (in THF) of compounds **5–8**. DFT calculations were performed at the B3LYP-D3(BJ)/def2-SVP level of theory.

about 10 kcal/mol (Scheme 6). However, our attempts to induce H_2 or HCl elimination by reaction with different Brønsted bases were once more unsuccessful furnishing decomposition instead the intended phosphagallene adducts.

Conclusions

In this contribution, we have presented eight derivatives of monomeric phophanylgallanes stabilized by a strong σ-donor, and sterically demanding Lewis base, namely 1,3-bis(2,6-diisopropylphenyl) imidazoline-2-ylidene. In addition to the species, which are only organosubstituted on the P atom, the parent compounds bearing *H,H* or *H,Cl*-functionalization were isolated coordinating to a Lewis base or a Lewis base/acid pair. The products were characterized by means of spectroscopy, single crystal X-ray diffraction and DFT methods. These compounds exhibit Ga–P bond lengths typical for a single bond and a slightly longer C_{carb}–Ga bond length than a single bond. The bonding analysis suggests a fairly stable interaction between the Lewis base and the phosphagallane, which is mainly dominated by the electrostatic interaction (> 50%). Notably, the introduction of a Lewis acid at the phosphorus lone pair enhances the bond energy by 10 kcal/mol which is mainly due to a stronger orbital interaction. The Lewis base and Lewis acid/base-stabilized species do not show reactivity towards Brønsted bases due to their high proton affinity.

Experimental Section

General considerations. All syntheses and manipulations were carried out under argon atmosphere (Ar), using either Schlenk line techniques or a glovebox (MBraun Unilan Plus). The glassware was pre-dried in oven at 125 °C and heated in *vacuo* prior to use. Organic solvents THF, benzene and *n*-pentane were taken directly from solvent purification system (Innovative Technology PureSolv MD5). Deuterated benzene was dried over appropriate drying agents, distilled and, stored inside a glovebox. NMR-spectra were recorded at 300 K on a Bruker Avance III 300 and a Bruker Avance IV HD 400 spectrometer. (^{1}H: 400.13 MHz,^{13}C: 100.61 MHz, ^{11}B: 128.38 MHz, ^{31}P: 121.5 MHz). Chemical shifts (in δ, ppm) are referenced to the residual solvent signal(s): C_6D_6 (^{1}H, 7.16; ^{13}C, 128.06).[34] Fourier-transform IR spectra were acquired on a Bruker Vertex 70 spectrometer in attenuated total reflectance (ATR) mode.

Elemental analyses were performed on an elemental analyzer Leco CHN-900 and/or an elementar 161vario Micro Cube. Single crystal X-ray diffraction analysis were carried out at low temperatures on Bruker AXS D8 Venture diffractometer operating with a microfocus sealed tube and a Photon II detector. Monochromated MoKa radiation (l = 0.71073 Å) was used. Structure solution and refinement were performed using SHELX.[35] These data can be obtained free of charge from The Cambridge Crystallographic Data Centre via http://www.ccdc.cam.ac.uk. ^{n}BuLi (1.6 M in hexane, Alfa-Aesar), GaCl$_3$ (Sigma Aldrich), and PhPH$_2$ (10% wt. in hexane) (ABCR GmbH) were commercially available and used without further purification. Phosphine-boranes RPH$_2$.BH$_3$,[31] LiPPh$_2$,[36] IDip.GaCl$_3$[37] and IDip.GaH$_2$Cl[38] were prepared according to the literature procedures.

Compound 1 (IDipGaCl$_2$PHPh): 10% weight in hexane solution of PhPH$_2$ (0.5 mL, 0.49 mmol) was added in 2 mL of THF and 1.6 M of ^{n}BuLi (0.3 mL, 0.49 mmol) was added dropwise to the solution at −78 °C. After stirring at −78 °C for 30 minutes, it was added dropwise to the THF solution of IDip.GaCl$_3$ (250 mg, 0.44 mmol) at −78 °C. Upon addition, volatiles were evaporated under vacuum. The product was then extracted with 8 mL of benzene. Benzene was then removed under reduced pressure and the residue was washed with *n*-pentane (2×5 mL), leading to mg (128 mg, 20%) of a white solid. Colourless crystals were grown by slow evaporation of saturated toluene solution at room temperature. ^{1}H NMR (400 MHz, C$_6$D$_6$) δ ppm: 7.59–7.54 (m, 1H, Ar), 7.32–7.18 (m, 6H, Ar), 7.14–7.07 (m, 4H, Ar), 6.44 (s, 2H, NC*H*), 2.76 (sep, 3H, C*H*(CH$_3$)$_2$), 2.71 (sep, 4H, C*H*(CH$_3$)$_2$), 2.66 (d, $^1J_{H,P}$ = 196.6 Hz P*H*Ph) 1.51–1.41 (m, 12H, CH(C*H$_3$)$_2$), 1–02–0.94 (m, 12H, CH(C*H$_3$)$_2$) ppm. ^{13}C{^{1}H} NMR (100.6 MHz, C$_6$D$_6$, 298 K): 168.1 (d, $^2J_{C,P}$ = 14.9 Hz, NCN), 146.2 (Ar), 146.0 (Ar), 145.8 (Ar), 135.0 (d, 15.03 Hz), 131.7 (Ar), 126.4 (Ar), 125.7 (Ar), 125.3 (Ar), 124.9 (Ar), 124.6 (d, 5.43 Hz), 29.2 (CH(CH$_3$)$_2$), 25.9 (CH(CH$_3$)$_2$, 23.1 (CH(CH$_3$)$_2$) ppm. ^{31}P NMR (161.9 MHz, C$_6$D$_6$, 298 K): −130.2 (d, $^1J_{P,H}$ = 197.0 Hz) ppm. **EA (%)**: calcd. C: 62.10 H: 6.63 N: 4.39; found: C: 62.57, H: 6.30, N: 4.00; **MP**: 187 °C(decomp.). **APPI-MS (***m/z***)**: 601.20 [M−Cl$^•$ + H]$^+$.

Compound 2 (IDipGaH$_2$PHPh). 10% weight in hexane solution of PhPH$_2$ (0.2 mL, 0.22 mmol) was added in 2 mL of THF and 1.6 M of ^{n}BuLi (0.1 mL, 0.22 mmol) was added dropwise to the solution at −78 °C. After stirring at −78 °C for 30 minutes, it was added dropwise to the THF solution of IDip.GaH$_2$Cl (100 mg, 0.20 mmol) at −78 °C. Upon addition, volatiles were evaporated under vacuum. The product was then extracted with 8 mL of benzene. Benzene was then removed under reduced pressure and the residue was washed with *n*-pentane (2 x 5 mL) to afford the product as white solid (59 mg, 51%). Colourless crystals were grown by slow evaporation of saturated benzene solution at room temperature. ^{1}H NMR (400 MHz, C$_6$D$_6$) δ ppm: 7.44–7.39 (m, 2H, Ar), 7.29–7.24 (m, 3H, Ar), 7.14–7-11 (m, 6H, Ar), 6.45 (s, 2H, NC*H*), 2.77 (dt, $^1J_{H,P}$ = 188.7 Hz, $^3J_{H,H}$ = 4.5 Hz 1H, P*H*Ph), 2.69 (sep, 4H, C*H*(CH$_3$)$_2$), 1.44 (d, 12H, CH(C*H$_3$)$_2$), 1.04 (d, 12H, CH(C*H$_3$)$_2$) ppm. ^{13}C{^{1}H} NMR (100.6 MHz, C$_6$D$_6$, 298 K): 179.2 (d, $^2J_{C,P}$ = 19.9 Hz, NCN), 145.7 (Ar), 142.5 (d, 20.9 Hz, Ar), 134.76 (Ar), 133.6 (d, 13.0 Hz, NCHCHN), 130.9 (Ar), 124.7 (d, 7.8 Hz, Ar), 124.4 (Ar), 124.1 (d, 6.22 Hz, Ar), 123.7 (d, 5.1 Hz, Ar), 29.1 (CH(CH$_3$)$_2$), 25.4 (CH(CH$_3$)$_2$), 23.2 (d, 3.3 Hz, (CH(CH$_3$)$_2$)) ppm. ^{31}P NMR (161.9 MHz, C$_6$D$_6$, 298 K): −142.7 (d, $^1J_{P,H}$ = 189.6 Hz, $^2J_{P,H}$ = 16.4 Hz) ppm. **EA (%)**: calcd. C: 69.61 H: 7.79 N: 4.92; found: C: 67.50, H: 7.22, N: 4.78; **MP**: 74 °C(decomp.). **APPI-MS (***m/z***)**: 567.24 [M]$^+$. Compound **2** consistently analyzed low for carbon over repeated analyses.

Compound 3 (IDipGaCl$_2$PPh$_2$). 5 mL THF solution of LiPPh$_2$ (70 mg, 0.36 mmol) was added dropwise to the solution of 5 mL THF solution of IDip.GaCl$_3$ (250 mg, 0.44 mmol) at −78 °C. Upon addition, volatiles were evaporated under vacuum. The product was then extracted with 8 mL of benzene. Benzene was then removed under reduced pressure and the remaining white solid is

EurJIC
European Journal of Inorganic Chemistry

Research Article
doi.org/10.1002/ejic.202200477

Chemistry Europe
European Chemical
Societies Publishing

washed with *n*-pentane (2×5 mL) to afford the product as white solid (97 mg, 34%). Colourless crystals were grown by slow evaporation of saturated benzene solution at room temperature. **¹H NMR (400 MHz, C₆D₆, 298 K):** 7.65–7.59 (m, 4H, Ar), 7.24–7.19 (m, 2H, Ar), 7.11–7.06 (m, 4H, Ar), 7.05–6.99 (m, 4H, Ar), 6.98–6.92 (m, 2H, Ar), 6.43 (s, 2H, NC*H*C*H*N), 2.85 (sep, 4H, C*H*(CH₃)₂), 1.40 (d, 12H, CH(C*H₃*)₂), 0.96 (d, 12H, CH(C*H₃*)₂) ppm. **¹³C{¹H} NMR (100.6 MHz, C₆D₆, 298 K):** 168.3 (d, $^2J_{C,P}$=27.3 Hz, NCN), 145.9 (Ar), 138.0 (d, 21.0 Hz, Ar), 135.9 (d, 19.4 Hz, Ar), 134.3 (Ar), 134.0 (Ar), 131.5 (Ar), 127.1 (Ar), 125.6 (Ar), 124.7 (Ar), 29.2 (*C*H(CH₃)₂), 26.2 (CH(*C*H₃)₂), 22.9 (CH(*C*H₃)₂) ppm. **³¹P NMR (161.9 MHz, C₆D₆, 298 K):** −51.7 ppm. **EA (%):** calcd. C: 65.57 H: 6.49 N: 3.92; found: C: 64.33, H: 6.10, N: 3.69; **MP:** 248 °C(decomp.). **APPI-MS (*m/z*):** 713.21 [M]⁺. Compound **3** consistently analyzed low for carbon over repeated analyses.

Compound **4** (IDipGaH₂PPh₂). 5 mL THF solution of LiPPh₂ (97 mg, 0.50 mmol) was added dropwise to the solution of 5 mL THF solution of IDip.GaH₂Cl (250 mg, 0.50 mmol) at −78 °C. Upon addition, volatiles were evaporated under vacuum. The product was then extracted with 8 mL of benzene. Benzene was then removed under reduced pressure and the remaining white solid is washed with *n*-pentane (2×5 mL) to afford the product as white solid (67 mg, 21%). Colourless crystals were grown by slow evaporation of saturated benzene solution at room temperature. **¹H NMR (400 MHz, C₆D₆) δ:** 7.45–7.40 (m, 4H, Ar), 7.24–7.19 (m, 2H, Ar), 7.10–7.06 (m, 4H, Ar), 7.03–6.98 (m, 4H, Ar), 6.95–6.88 (m, 2H, Ar), 6.48 (s, 2H, NC*H*C*H*N), 4.23 (d, $^2J_{P,H}$=13.3 Hz, GaH₂), 2.75 (sep, 4H, C*H*(CH₃)₂), 1.38 (d, 12H, CH(C*H₃*)₂), 1.01 (d, 12H, CH(C*H₃*)₂) ppm. **¹³C{¹H} NMR (100.6 MHz, C₆D₆, 298 K):** 178.8 (d, $^2J_{C,P}$=28.1 Hz, NCN), 145.6 (Ar), 144.4 (Ar), 144.2 (Ar), 134.9 (d, 16.5 Hz, Ar), 130.9, 127.7 (d, 5.8 Hz, Ar), 125.2 (Ar), 128.8 (d, 6.0 Hz, Ar), 124.4 Hz (Ar), 29.1 (*C*H(CH₃)₂), 25.5 (CH(*C*H₃)₂), 23.0 (CH(*C*H₃)₂) ppm. **³¹P NMR (161.9 MHz, C₆D₆, 298 K):** −59.1 ppm. **EA (%):** calcd. C: 72.57 H: 7.50 N: 4.34; found: C: 69.98, H: 6.58, N: 3.71; **MP:** 196 °C(decomp.). **APPI-MS (*m/z*):** 643.27 [M]⁺. Compound **4** consistently analyzed low for carbon over repeated analyses.

Compound **5** (IDipGaCl₂PHNCy₂.BH₃). (NCy₂)PH₂.BH₃ (111 mg, 0.49 mmol) was dissolved in 3 mL of dry THF and cooled down to −78 °C. To this solution, 1.6 M of ⁿBuLi (0.3 mL, 0.49 mmol) solution in hexane was added dropwise. After stirring at −78 °C for 30 minutes, it was added dropwise to the THF solution of IDip.GaCl₃ (278 mg, 0.44 mmol) at −78 °C. After the addition is complete, volatiles were under vacuum. The products were then extracted with 10 mL of benzene and washed with *n*-pentane (2×10 mL) to yield the product as white powder (128 mg, 34%). Single crystals were grown by slow evaporation of saturated benzene solution at room temperature. **¹H NMR (400 MHz, C₆D₆, 298 K):** 7.28–7.24 (m, 3H, Ar), 7.14–7.11(m, 3H, Ar), 6.51 (s, 2H, NC*H*), 5.32 (dq, $^1J_{H,P}$=339.8 Hz, $^3J_{H,H}$=7.3 Hz 1H, −P*H*), 3.00–2.90 (m, 2H, Cy*H*), 2.82 (sep, 4H, C*H*(CH₃)₂), 1.97–1.79 (m, 6H, Cy*H*), 1.60–1.51 (m, 17H, CH(C*H₃*)₂, Cy*H*), 1.44–1.40 (m, 4H, Cy*H*), 0.99–0.92 (m, 17H, CH(C*H₃*)₂, Cy*H*) δ ppm. **¹³C{¹H} NMR (100.6 MHz, C₆D₆, 298 K):** 165.8 (d, $^2J_{C,P}$=32.0, NCN), 146.4 (d, 48.6 Hz, Ar), 133.8 (Ar), 131.8 (Ar), 126.0 (Ar), 124.6 (d, 26.7 Hz, Ar), 57.1 (d, 3.5 Hz, NCHCH₂), 33.9 (NCHCH₂*C*H₂CH₂), 33.1(NCHCH₂CH₂*C*H₂), 29.3 (d, 19.9 Hz, NCHCH₂*C*H₂CH₂), 26.6 (d, 4.2 Hz, NCHCH₂CH₂*C*H₂), 26.3 (d, 19.6 Hz, CH(*C*H₃)₂), 26.0 (CH(*C*H₃)₂), 23.0 (d, 22.1 Hz, CH(*C*H₃)₂) δ ppm. **³¹P NMR (161.9 MHz, C₆D₆, 298 K):** −2.9 ppm (bd, $^1J_{P,H}$=342.4 Hz), **¹¹B{¹H} NMR (128.4 MHz, C₆D₆, 298 K) δ:** −34.1 ppm. **EA (%):** calcd. C:62.01 H:8.27 N:5.56; found: C:62.05, H:7.77, N:5.13. **MP:** 108 °C(decomp.).

Compound **6** (IDipGaCl₂PHNiPr₂.BH₃). (NiPr₂)PH₂.BH₃ (65 mg, 0.43 mmol) was dissolved in 3 mL of dry THF and cooled down to −78 °C. To this solution, 1.6 M of ⁿBuLi (0.3 mL, 0.48 mmol) solution in hexane was added dropwise. After stirring at −78 °C for 30 minutes, it was added dropwise to the THF solution of IDip.GaCl₃ (250 mg, 0.44 mmol) at −78 °C. After the addition is complete, volatiles were

under vacuum. The products were then extracted with 10 mL of benzene and washed with *n*-pentane (2×10 mL) to yield the product as white powder (124 mg, 41%). Single crystals were grown by slow evaporation of saturated benzene solution at room temperature. **¹H NMR (400 MHz, C₆D₆, 298 K) δ ppm:** 7.27–7.23 (m, 2H, Ar), 7.15–1.11 (m, 4H, Ar), 5.28 (dq, $^1J_{H,P}$=337.0 Hz, $^3J_{H,H}$=7.3 Hz,1H, −P*H*), 3.33 (sep, 2H, C*H*(CH₃)₂), 2.95–2.73 (m, 4H, C*H*(CH₃)₂), 1.57 (t, 12H, CH(C*H₃*)₂), 1.03 (d, 6H, CH(C*H₃*)₂), 0.96 (t, 18H, CH(C*H₃*)₂) ppm. **¹³C{¹H} NMR (100.6 MHz, C₆D₆, 298 K):** 146.4 (d, $^2J_{C,P}$=38.7 Hz, NCN), 133.8 (Ar), 131.7 (Ar), 126.0 (Ar), 124.6 (d, 24.7 Hz, Ar), 48.2 (d, 3.96 Hz, NCHCH₂), 29.3 (d, 16.8 Hz, *C*H(CH₃)₂), 26.3 (d, 13.5 Hz, CH(*C*H₃)₂), 23.1 (d, 10.3 Hz, CH(*C*H₃)₂), 22.8 (d, 2.4 Hz, NC*H*(CH₃)₂), 22.5 (d, 2.7 Hz, NCH(*C*H₃)₂) δ ppm. **³¹P NMR (161.9 MHz, C₆D₆, 298 K):** −6.7 (bd, $^1J_{P,H}$=339.1 Hz) ppm. **¹¹B{¹H} NMR (128.4 MHz, C₆D₆, 298 K) δ:** −34.2 ppm. **EA (%):** calcd. C:58.70 H:8.06 N: 6.22; found: C:57.27, H:7.77, N:5.86; **MP:** 132 °C(decomp.) Compound **6** consistently analyzed low for carbon over repeated analyses.

Compound **7** (IDipGaH₂PHTip.BH₃). TipPH₂.BH₃ (41 mg, 0.16 mmol) was dissolved in 3 mL of dry THF and cooled down to −78 °C. To this solution, 1.6 M of ⁿBuLi (0.1 mL, 0.16 mmol) solution in hexane was added dropwise. After stirring at −78 °C for 30 minutes, it was added dropwise to the THF solution of IDip.GaH₂Cl (100 mg, 0.20 mmol) at −78 °C. After the addition is complete, volatiles were under vacuum. The products were then extracted with 10 mL of benzene and washed with *n*-pentane (2×10 mL) to yield the product as white powder (30 mg, 26%). Single crystals were grown by vapour diffusion into a saturated toluene solution at room temperature. **¹H NMR (400 MHz, C₆D₆, 298 K) δ ppm:** 7.29–7.21 (m, 2H, Ar), 7.15–7.09 (m, 4H, Ar), 7.02 (s, 2H, Ar), 6.50 (s, 2H, NC*H*), 4.28 (d*t*, $^1J_{H,P}$=310.2 Hz, $^3J_{H,H}$=7.0 Hz 1H, -P*H*), 3.31 (sept, 2H, C*H*(CH₃)₂), 2.93 (sept, 2H, C*H*(CH₃)₂), 2.77–2.51 (m, 3H, C*H*(CH₃)₂), 1.45 (d, 12H, CH(C*H₃*)₂), 1.31 (d, 6H, CH(C*H₃*)₂), 1.24 (d, 6H, CH(C*H₃*)₂), 1.12 (d, 6H, CH(C*H₃*)₂), 1.04–0.93 (m, 12H, CH(C*H₃*)₂) ppm. **¹³C{¹H} NMR (100.6 MHz, C₆D₆, 298 K):** 174.8 (d, $^2J_{C,P}$=13.1 Hz, NCN), 152.1 (d, 8.4 Hz, Ar),148.4 (d, 2.4 Hz, Ar), 145.9 (d, 17.5 Hz, Ar), 134.7 (Ar), 131.1 (Ar), 125.0 (Ar), 124.6 (Ar), 124.4 (Ar), 121.7 (d, 7.0 Hz, Ar), 34.5 (*C*H(CH₃)₂), 32.7 (d, 8.2 Hz, *C*H(CH₃)₂), 29.0 (d, 22.1 Hz, *C*H(CH₃)₂), 25.9 (CH(*C*H₃)₂), 25.7 (d, 15.0 Hz, CH(*C*H₃)₂), 24.7 (CH(*C*H₃)₂), 24.1 (d, 3.6 Hz, CH(*C*H₃)₂), 23.5 (CH(*C*H₃)₂), 23.0 (CH(*C*H₃)₂) ppm. **³¹P NMR (161.9 MHz, C₆D₆, 298 K):** −110.7 (bd, $^1J_{P,H}$=309.4 Hz) ppm. **¹¹B{¹H} NMR (128.4 MHz, C₆D₆, 298 K):** −33.10 δ ppm. **EA (%):** calcd. C:71.10 H:9.23 N:3.95 ; found: C:67.17, H:7.96, N:3.55; **MP:** 180 °C-(decomp.). **APPI-MS (*m/z*):** 693.38 [M-BH₃]⁺. Compound **7** consistently analyzed low for carbon over repeated analyses.

Compound **8** (IDipGaH₂PHMes.BH₃). MesPH₂.BH₃ (83.7 mg, 0.50 mmol) was dissolved in 3 mL of dry THF and cooled down to −78 °C. To this solution, 1.6 M of ⁿBuLi (0.4 mL, 0.64 mmol) solution in hexane was added dropwise. After stirring at −78 °C for 30 minutes, it was added dropwise to the THF solution of IDip.GaH₂Cl (250 mg, 0.50 mmol) at −78 °C. After the addition is complete, volatiles were under vacuum. The products were then extracted with 10 mL of benzene and washed with *n*-pentane (2×10 mL) to yield the product as white powder (97 mg, 31%). Single crystals were grown by slow evaporation of saturated benzene solution at room temperature. **¹H NMR (400 MHz, C₆D₆) δ ppm:** 7.26–7.21 (m, 3H), 7.13–7.09 (m, 5H), 6.48 (s, 2H), 2.88 (sept, 2H), 2.68 (sept, 2H), 2.34 (s, 6H), 1.96 (s, 3H), 1.48–1.44 (m, 12H), 1.01–0.95 (m, 12H) ppm. **¹³C{¹H} NMR (100.6 MHz, C₆D₆, 298 K):**174.4 (d, $^2J_{C,P}$=10.2 Hz. NCN), 145.9 (Ar, d, 18.0 Hz), 141.1.1 (Ar, d, 7.2 Hz), 136.9 (Ar), 134.6 (Ar), 131.2 (Ar), 129.2 (Ar, d, 7.1 Hz), 125.1 (Ar), 124.7 (Ar), 124.4 (Ar), 34.4 (NCHCH₂), 29.2 (*C*H(CH₃)₂, d, 15.0), 25.7 (*o*-PhCH₃, d, 23.5 Hz), 23.6 (*p*-PhCH₃, d, 6.0 Hz), 23.4 (CH(*C*H₃)₂), 23.1 ppm (CH(*C*H₃)₂). **³¹P NMR (161.9 MHz, C₆D₆, 298 K):** −103.5 ppm (d, $^1J_{P,H}$=316.8 Hz) ppm. **¹¹B{¹H} NMR (128.4 MHz, C₆D₆, 298 K):** −35.1 δ ppm. **EA (%):** calcd. C:69.15 H:8.54 N:4.48; found: C:67.01, H:7.31, N:3.83; **MP:**

98 °C(decomp.). APPI-MS (*m/z*): 609.29 [M-BH$_3$]$^+$. Compound **8** consistently analyzed low for carbon over repeated analyses.

Computational Details. All geometry optimizations were performed using the Gaussian 16.C01 software.[39] All geometry optimizations were computed using the functional B3LYP[40] functional with Grimme dispersion corrections D3[41] and the Becke-Jonson damping function[42] in combination with the def2-SVP basis set.[43] The stationary points were located with the Berny algorithm[44] using redundant internal coordinates. Analytical Hessians were computed to determine the nature of stationary points (one and zero imaginary frequencies for transition states and minima, respectively)[45] and to calculate unscaled zero-point energies (ZPEs) as well as thermal corrections and entropy effects using the standard statistical-mechanics relationships for an ideal gas.

The atomic partial charges were estimated with the natural bond orbital (NBO)[22] method using NBO 7.0.[46] The topological quantum theory of atoms in molecules (QTAIM),[24] and Laplacian of the electron density analyses were carried out with AIMAII.[47] The calculations were performed at the B3LYP-D3(BJ)/def2-TZVPP level of theory.

The nature of the chemical bonds were investigated by means of the Energy Decomposition Analysis (EDA) method, which was developed by Morokuma[48] and by Ziegler and Rauk.[49] The bonding analysis focuses on the instantaneous interaction energy ΔE_{int} of a bond A–B between two fragments A and B in the particular electronic reference state and in the frozen geometry AB. This energy is divided into four main components (Eq 1).

$$\Delta E_{int} = \Delta E_{elst} + \Delta E_{Pauli} + \Delta E_{orb} + \Delta E_{disp} \qquad (1)$$

The term ΔE_{elst} corresponds to the classical electrostatic interaction between the unperturbed charge distributions of the prepared atoms (or fragments) and it is usually attractive. The Pauli repulsion ΔE_{Pauli} is the energy change associated with the transformation from the superposition of the unperturbed wave functions (Slater determinant of the Kohn-Sham orbitals) of the isolated fragments to the wave function $\Psi^0 = N\hat{A}[\Psi_A\Psi_B]$, which properly obeys the Pauli principle through explicit antisymmetrization (Â operator) and renormalization (N = constant) of the product wave function. It comprises the destabilizing interactions between electrons of the same spin on either fragment. The orbital interaction ΔE_{orb} accounts for charge transfer and polarization effects.[50] In the case that the Grimme dispersion corrections[41–42] are computed the term ΔE_{disp} is added to equation 1. Further details on the EDA method can be found in the literature.[51] In the case of the dimers, relaxation of the fragments to their equilibrium geometries at the electronic ground state is termed ΔE_{prep}, because it may be considered as preparation energy for chemical bonding. The addition of ΔE_{prep} to the intrinsic interaction energy ΔE_{int} gives the total energy ΔE, which is, by definition, the opposite sign of the bond dissociation energy D_e:

$$\Delta E(-D_e) = \Delta E_{int} + \Delta E_{prep} \qquad (2)$$

The EDA–NOCV method combines the EDA with the natural orbitals for chemical valence (NOCV) to decompose the orbital interaction term ΔE_{orb} into pairwise contributions. The NOCVs Ψ_i are defined as the eigenvector of the valence operator, $\hat{V}$, given by Equation (3).

$$\bar{V}\,\Psi_i = \nu_i\Psi_i \qquad (3)$$

In the EDA–NOCV scheme the orbital interaction term, ΔE_{orb}, is given by Equation (4),

$$\Delta E_{orb} = \sum_k \Delta E_k = \sum_{k=1}^{N/2} \nu_k \left[-F_{-k,k}^{TS} + -F_{k,k}^{TS} \right] \qquad (4)$$

in which $F_{-k,-k}^{TS}$ and $F_{k,k}^{TS}$ are diagonal transition state Kohn–Sham matrix elements corresponding to NOCVs with the eigenvalues $-\nu_k$ and ν_k, respectively. The ΔE_k^{orb} term for a particular type of bond is assigned by visual inspection of the shape of the deformation density $\Delta\rho_k$. The latter term is a measure of the size of the charge deformation and it provides a visual notion of the charge flow that is associated with the pairwise orbital interaction. The EDA-NOCV scheme thus provides both qualitative and quantitative information about the strength of orbital interactions in chemical bonds. The EDA-NOCV calculations were carried out with ADF2019. The basis sets for all elements have triple-ζ quality augmented by two sets of polarizations functions and one set of diffuse function. Core electrons were treated by the frozen-core approximation. This level of theory is denoted BP86-D3(BJ)/TZ2P.[52] Scalar relativistic effects have been incorporated by applying the zeroth-order regular approximation (ZORA).[53]

Deposition Numbers 2182156 (for **1**), 2182157 (for **2**), 2182158 (for **3**), 2182159 (for **4**), 2182160 (for **5**), 2182162 (for **6**), 2182163 (for **7**), 2182165 (for **8**) contain the supplementary crystallographic data for this paper. These data are provided free of charge by the joint Cambridge Crystallographic Data Centre and Fachinformationszentrum Karlsruhe Access Structures service www.ccdc.cam.ac.uk/structures.

Conflict of Interest

The authors declare no conflict of interest.

Data Availability Statement

The data that support the findings of this study are available in the supplementary material of this article.

[1] a) F. Dimroth, *Phys. Status Solidi C* **2006**, *3*, 373–379; b) A. M. Glass, *Science* **1987**, *235*, 1003–1009.

[2] a) A. H. Cowley, R. A. Jones, *Angew. Chem. Int. Ed. Engl.* **1989**, *28*, 1208–1215; b) D. A. Neumayer, A. H. Cowley, A. Decken, R. A. Jones, V. Lakhotia, J. G. Ekerdt, *J. Am. Chem. Soc.* **1995**, *117*, 5893–5894; c) F. Maury, *Adv. Mater.* **1991**, *3*, 542–548; d) R. L. Wells, W. L. Gladfelter, *J. Cluster Sci.* **1997**, *8*, 217–238.

EurJIC
European Journal of Inorganic Chemistry

Research Article
doi.org/10.1002/ejic.202200477

Chemistry
Europe
European Chemical
Societies Publishing

[3] S. Schulz, in *Advances in Organometallic Chemistry, Vol 49, Vol. 49* (Eds.: R. West, A. F. Hill), **2003**, pp. 225–317.

[4] a) R. T. Paine, H. Noth, *Chem. Rev.* **1995**, *95*, 343–379; b) F. A. Cotton, A. H. Cowley, X. J. Feng, *J. Am. Chem. Soc.* **1998**, *120*, 1795–1799; c) R. J. Wright, A. D. Phillips, T. L. Allen, W. H. Fink, P. P. Power, *J. Am. Chem. Soc.* **2003**, *125*, 1694–1695; d) G. He, O. Shynkaruk, M. W. Lui, E. Rivard, *Chem. Rev.* **2014**, *114*, 7815–7880; e) F. Dankert, C. Hering-Junghans, *Chem. Commun.* **2022**, *58*, 1242–1262; f) M. Fischer, S. Nees, T. Kupfer, J. T. Goettel, H. Braunschweig, C. Hering-Junghans, *J. Am. Chem. Soc.* **2021**, *143*, 4106–4111; g) S. Nees, F. Fantuzzi, T. Wellnitz, M. Fischer, J. E. Siewert, J. T. Goettel, A. Hofmann, M. Harterich, H. Braunschweig, C. Hering-Junghans, *Angew. Chem. Int. Ed.* **2021**, *60*, 24318–24325.

[5] a) P. P. Power, *Chem. Rev.* **1999**, *99*, 3463–3504; b) R. C. Fischer, P. P. Power, *Chem. Rev.* **2010**, *110*, 3877–3923; c) P. P. Power, *Acc. Chem. Res.* **2011**, *44*, 627–637.

[6] E. Rivard, *Dalton Trans.* **2014**, *43*, 8577–8586.

[7] W. Haider, M. D. Calvin-Brown, I.-A. Bischoff, V. Huch, B. Morgenstern, C. Müller, T. Sergeieva, D. M. Andrada, A. Schäfer, *Inorg. Chem.* **2022**, *61*, 1672–1684.

[8] a) F. Thomas, S. Schulz, M. Nieger, *Eur. J. Inorg. Chem.* **2001**, 161–166; b) A. Kuczkowski, F. Thomas, S. Schulz, M. Nieger, *Organometallics* **2000**, *19*, 5758–5762; c) S. Schulz, M. Nieger, *Organometallics* **2000**, *19*, 2640–2642.

[9] F. Thomas, S. Schulz, M. Nieger, K. Nättinen, *Chem. Eur. J.* **2002**, *8*, 1915–1924.

[10] a) M. Balmer, M. Kapitein, C. von Hänisch, *Dalton Trans.* **2017**, *46*, 7074–7081; b) M. Kapitein, M. Balmer, L. Niemeier, C. von Hänisch, *Dalton Trans.* **2016**, *45*, 6275–6281; c) M. Kapitein, M. Balmer, C. von Hänisch, *Z. Anorg. Allg. Chem.* **2016**, *642*, 1275–1281; d) M. Kapitein, M. Balmer, C. von Hänisch, *Phosphorus Sulfur Silicon Relat. Elem.* **2016**, *191*, 641–644; e) M. Kapitein, C. von Hänisch, *Eur. J. Inorg. Chem.* **2015**, 837–844.

[11] U. Vogel, A. Y. Timoshkin, M. Scheer, *Angew. Chem. Int. Ed.* **2001**, *40*, 4409–4412; *Angew. Chem.* **2001**, *113*, 4541–4544.

[12] a) M. Bodensteiner, A. Y. Timoshkin, E. V. Peresypkina, U. Vogel, M. Scheer, *Chem. Eur. J.* **2013**, *19*, 957–963; b) M. Bodensteiner, U. Vogel, A. Y. Timoshkin, M. Scheer, *Angew. Chem. Int. Ed.* **2009**, *48*, 4629–4633; *Angew. Chem.* **2009**, *121*, 4700–4704; c) U. Vogel, P. Hoemensch, K. C. Schwan, A. Y. Timoshkin, M. Scheer, *Chem. Eur. J.* **2003**, *9*, 515–519; d) U. Vogel, A. Y. Timoshkin, K. C. Schwan, M. Bodensteiner, M. Scheer, *J. Organomet. Chem.* **2006**, *691*, 4556–4564; e) M. A. K. Weinhart, A. S. Lisovenko, A. Y. Timoshkin, M. Scheer, *Angew. Chem. Int. Ed.* **2020**, *59*, 5541–5545; *Angew. Chem.* **2020**, *132*, 5586–5590; f) M. A. K. Weinhart, M. Seidl, A. Y. Timoshkin, M. Scheer, *Angew. Chem. Int. Ed.* **2021**, *60*, 3806–3811; *Angew. Chem.* **2021**, *133*, 3850–3855; g) E. Leiner, M. Scheer, *Organometallics* **2002**, *21*, 4448–4453; h) U. Vogel, K. C. Schwan, M. Scheer, *Eur. J. Inorg. Chem.* **2004**, 2062–2065.

[13] a) M. L. Cole, S. K. Furfari, M. Kloth, *J. Organomet. Chem.* **2009**, *694*, 2934–2940; b) S. G. Alexander, M. L. Cole, S. K. Furfari, M. Kloth, *Dalton Trans.* **2009**, 2909–2911; c) A. Hock, L. Werner, C. Luz, U. Radius, *Dalton Trans.* **2020**, *49*, 11108–11119.

[14] a) V. Nesterov, D. Reiter, P. Bag, P. Frisch, R. Holzner, A. Porzelt, S. Inoue, *Chem. Rev.* **2018**, *118*, 9678–9842; b) M. M. D. Roy, A. A. Omaña, A. S. S. Wilson, M. S. Hill, S. Aldridge, E. Rivard, *Chem. Rev.* **2021**, *121*, 12784–12965.

[15] A. K. Swarnakar, M. J. Ferguson, R. McDonald, E. Rivard, *Dalton Trans.* **2017**, *46*, 1406–1412.

[16] a) T. Agou, S. Ikeda, T. Sasamori, N. Tokitoh, *Eur. J. Inorg. Chem.* **2018**, *2018*, 1984–1987; b) T. Agou, S. Ikeda, T. Sasamori, N. Tokitoh, *Eur. J. Inorg. Chem.* **2016**, 623–627.

[17] X. Bantreil, S. P. Nolan, *Nat. Protoc.* **2011**, *6*, 69–77.

[18] P. L. Baxter, A. J. Downs, D. W. H. Rankin, *J. Chem. Soc. Dalton Trans.* **1984**, 1755–1758.

[19] M. D. Francis, D. E. Hibbs, M. B. Hursthouse, C. Jones, N. A. Smithies, *J. Chem. Soc. Dalton Trans.* **1998**, 3249–3254.

[20] P. Pyykko, *J. Chem. Phys. A* **2015**, *119*, 2326–2337.

[21] L. L. Zhao, M. von Hopffgarten, D. M. Andrada, G. Frenking, *WIREs Comput. Mol. Sci.* **2018**, *8*, e13450.

[22] a) A. E. Reed, R. B. Weinstock, F. Weinhold, *J. Chem. Phys.* **1985**, *83*, 735–746; b) A. E. Reed, L. A. Curtiss, F. Weinhold, *Chem. Rev.* **1988**, *88*, 899–926.

[23] J. Emsley, *The elements*, Clarendon Press; Oxford University Press, Oxford; New York, **1998**.

[24] R. F. W. Bader, *Atoms in Molecules: A Quantum Theory*, Clarendon, Oxford, **1990**.

[25] S. Dutta, S. M. De, S. Bose, E. Mahal, D. Koley, *Eur. J. Inorg. Chem.* **2020**, 638–655.

[26] a) W. Haider, D. M. Andrada, I.-A. Bischoff, V. Huch, A. Schäfer, *Dalton Trans.* **2019**, *48*, 14953–14957; b) T. Yang, D. M. Andrada, G. Frenking, *Mol. Phys.* **2019**, *117*, 1306–1314; c) D. M. Andrada, C. Foroutan-Nejad, *Phys. Chem. Chem. Phys.* **2020**, *22*, 22459–22464.

[27] J. Poater, D. M. Andrada, M. Solà, C. Foroutan-Nejad, *Phys. Chem. Chem. Phys.* **2022**, *24*, 2344–2348.

[28] P. Erdmann, L. Greb, *Angew. Chem. Int. Ed.* **2022**, *61*, e202114550.

[29] M. Blum, J. Kappler, S. H. Schlindwein, M. Nieger, D. Gudat, *Dalton Trans.* **2018**, *47*, 112–119.

[30] a) N. Takagi, G. Frenking, *Theor. Chem. Acc.* **2011**, *129*, 615–623; b) N. Takagi, T. Shimizu, G. Frenking, *Chem. Eur. J.* **2009**, *15*, 8593–8604; c) N. Takagi, T. Shimizu, G. Frenking, *Chem. Eur. J.* **2009**, *15*, 3448–3456; d) N. Takagi, R. Tonner, G. Frenking, *Chem. Eur. J.* **2012**, *18*, 1772–1780; e) S. Klein, R. Tonner, G. Frenking, *Chem. Eur. J.* **2010**, *16*, 10160–10170.

[31] G. B. de Jong, N. Ortega, M. Lutz, K. Lammertsma, J. C. Slootweg, *Chem. Eur. J.* **2020**, *26*, 15944–15952.

[32] M. M. D. Roy, E. Rivard, *Acc. Chem. Res.* **2017**, *50*, 2017–2025.

[33] E. Buncel, I. H. Um, *Tetrahedron* **2004**, *60*, 7801–7825.

[34] G. R. Fulmer. A. J. M. Miller, N. H. Sherden, H. E. Gottlieb, A. Nudelman, B. M. Stoltz, J. E. Bercaw, K. I. Goldberg, *Organometallics* **2010**, *29*, 2176–2179.

[35] a) G. M. Sheldrick, *Acta Crystallogr. Sect. A* **2008**, *64*, 112–122; b) G. M. Sheldrick, *Acta Crystallogr. Sect. C* **2015**, *71*, 3–8.

[36] P. W. Clark, *Org. Prep. Proced. Int.* **1979**, *11*, 103–106.

[37] N. Marion, E. C. Escudero-Adán, J. Benet-Buchholz, E. D. Stevens, L. Fensterbank, M. Malacria, S. P. Nolan, *Organometallics* **2007**, *26*, 3256–3259.

[38] A. Hock, L. Werner, C. Luz, U. Radius, *Dalton Trans.* **2020**, *49*, 11108–11119.

[39] M. J. Frisch, G. W. Trucks, H. B. Schlegel, G. E. Scuseria, M. A. Robb, J. R. Cheeseman, G. Scalmani, V. Barone, G. A. Petersson, H. Nakatsuji, X. Li, M. Caricato, A. V. Marenich, J. Bloino, B. G. Janesko, R. Gomperts, B. Mennucci, H. P. Hratchian, J. V. Ortiz, A. F. Izmaylov, J. L. Sonnenberg, D. Williams-Young, F. Ding, F. Lipparini, F. Egidi, J. Goings, B. Peng, A. Petrone, T. Henderson, D. Ranasinghe, V. G. Zakrzewski, J. Gao, N. Rega, G. Zheng, W. Liang, M. Hada, M. Ehara, K. Toyota, R. Fukuda, J. Hasegawa, M. Ishida, T. Nakajima, Y. Honda, O. Kitao, H. Nakai, T. Vreven, K. Throssell, J. J. A. Montgomery, J. E. Peralta, F. Ogliaro, M. J. Bearpark, J. J. Heyd, E. N. Brothers, K. N. Kudin, V. N. Staroverov, T. A. Keith, R. Kobayashi, J. Normand, K. Raghavachari, A. P. Rendell, J. C. Burant, S. S. Iyengar, J. Tomasi, M. Cossi, J. M. Millam, M. Klene, C. Adamo, R. Cammi, J. W. Ochterski, R. L. Martin, K. Morokuma, O. Farkas, J. B. Foresman, D. J. Fox, Gaussian 16, Revision C.01. Gaussian, Inc., Wallingford CT, **2019**.

[40] a) A. D. Becke, *J. Chem. Phys.* **1993**, *98*, 5648–5652; b) C. Lee, W. Yang, R. G. Parr, *Phys. Rev. B* **1988**, *37*, 785–789.

[41] S. Grimme, J. Antony, S. Ehrlich, H. Krieg, *J. Chem. Phys.* **2010**, *132*.

[42] S. Grimme, S. Ehrlich, L. Goerigk, *J. Comb. Chem.* **2011**, *32*, 1456–1465.

[43] F. Weigend, R. Ahlrichs, *Phys. Chem. Chem. Phys.* **2005**, *7*, 3297–3305.

[44] C. Y. Peng, P. Y. Ayala, H. B. Schlegel, M. J. Frisch, *J. Comb. Chem.* **1996**, *17*, 49–56.

[45] J. W. McIver, A. Komornic, *J. Am. Chem. Soc.* **1972**, *94*, 2625–2633.

[46] E. D. Glendening, C. R. Landis, F. Weinhold, *J. Comb. Chem.* **2019**, *40*, 2234–2241.

[47] T. A. Keith, T. K. Gristmill, 19.02.13 ed., Overland Park KS, USA (aim.tkgristmill.com), **2019**.

[48] K. Morokuma, *J. Chem. Phys.* **1971**, *55*, 1236–1244.

[49] a) T. Ziegler, A. Rauk, *Inorg. Chem.* **1979**, *18*, 1558–1565; b) T. Ziegler, A. Rauk, *Inorg. Chem.* **1979**, *18*, 1755–1759.

[50] F. M. Bickelhaupt, N. M. M. Nibbering, E. M. Van Wezenbeek, E. J. Baerends, *J. Phys. Chem.* **1992**, *96*, 4864–4873.

[51] a) F. M. Bickelhaupt, E. J. Baerends, in *Reviews in Computational Chemistry, Vol. 15* (Eds.: K. B. Lipkowitz, D. B. Boyd), **2000**, pp. 1–86; b) G. te Velde, F. M. Bickelhaupt, E. J. Baerends, C. Fonseca Guerra, S. J. A. van Gisbergen, J. G. Snijders, T. Ziegler, *J. Comb. Chem.* **2001**, *22*, 931–967.

[52] J. Krijn, E. J. Baerends, *Fit Functions in the HFS-Method* **1984**.

[53] E. Van Lenthe, E. J. Baerends, J. G. Snijders, *J. Chem. Phys.* **1993**, *99*, 4597–4610.